On the Diagram for the Onset of Global Chaos and Reconnection Phenomena in the Quadratic Nontwist Map

Susumu Shinohara and Yoji Aizawa

Department of Applied Physics, Waseda University, Tokyo 169-8555, Japan

The quadratic nontwist map is studied by defining the "indicator points" for the phase space. The indicator points enable us to obtain useful information concerning the onset of global chaos and reconnection phenomena. The diagram obtained by using the indicator points clearly reveals the effects of the reconnection phenomena on the transition to global chaos. A discussion is given of the last KAM curve for the quadratic nontwist map.

§1. Introduction

In this paper, we consider area-preserving maps that violate the twist condition. They are often called area-preserving "nontwist" maps. Violation of the twist condition is encountered in models from a variety of fields such as fluid dynamics, plasma physics, celestial mechanics, etc. Moreover, violation of the twist condition generically occurs in the neighborhood of tripling bifurcations of a Hamiltonian system.[5),11)]

Originally, the twist condition is assumed in order to prove important theorems concerning the persistence of KAM curves, e.g. the Moser twist theorem[1)] and the Aubry-Mather theorem.[2)] However, the precise effects of violation of the twist condition on the persistence of KAM curves have not yet been elucidated. Numerical studies of nontwist systems revealed that violation of the twist condition generally leads to complicated phase space phenomena, called reconnection phenomena.[3)-11)] The reconnection phenomena drastically change the phase space structure and thus strongly influence the breakup process of KAM curves.

In order to study in detail the properties arising from violation of the twist condition, we focus here on the quadratic nontwist map (QNM), which is one of the simplest prototypes of an area-preserving nontwist map. Previously, we showed that the onset of global chaos and the reconnection phenomena in the QNM could be systematically studied by defining the "indicator points" for the phase space. After summarizing the properties of the indicator points, we present the diagram for the onset of global chaos and reconnection phenomena. The diagram clearly reveals how reconnection phenomena influence the transition to global chaos. On the basis of the numerical results obtained by using the indicator points, a discussion is given of the last KAM curve for the QNM.

§2. The quadratic nontwist map

The QNM is defined by

$$T : \begin{cases} I_{n+1} = I_n - K\sin(\theta_n) \\ \theta_{n+1} = \theta_n + f(I_{n+1}) \pmod{2\pi}, \end{cases} \tag{1a}$$

$$f(I) = 2\pi\mu - I^2, \tag{1b}$$

where μ and K are parameters. Since the twist function $f(I)$ is quadratic, the mapping T does not satisfy the twist condition

$$\frac{df}{dI} \neq 0, \ \forall I. \tag{2}$$

In general, the quadratic twist function can be written as $f(I) = a_2 I^2 + a_1 I + a_0$, where a_2, a_1, a_0 are parameters. However, this form can be transformed into a form of Eq. (1b) by rescaling the parameters and variables as follows:

$$\sqrt{a_2}\left(I + \frac{a_1}{2a_2}\right) \to I, \quad \sqrt{a_2}\,K \to K, \quad \left(a_0 - \frac{a_1^2}{4a_2}\right) \to 2\pi\mu. \tag{3}$$

We adopt here a form of Eq. (1b), for which the twist condition fails at $I = 0$ for any value of μ in the integrable limit ($K = 0$).

Note that the mapping T is invariant under each of the following two transformations:

$$\mu \mapsto \mu + 1, \quad (K, I) \mapsto (-K, -I). \tag{4}$$

Therefore, it is sufficient to consider the parameter regions defined by

$$-0.5 \leq \mu < 0.5, \quad 0 \leq K < \infty. \tag{5}$$

Here we briefly summarize the phase space structures which are peculiar to nontwist systems. Figures 1(a) and (b) show, respectively, a phase space portrait of the QNM and its rotation number profile along the I-axis. Because of violation of the twist condition, the rotation number takes a maximum value at $I \simeq 0$. The KAM curve having the maximum rotation number is called the "shearless KAM curve". On either side of the shearless KAM curve, there exists an island chain with the same rotation number. They are often called "twin chains". As the parameters are varied, the twin chains exhibit reconnection phenomena. That is, the separatrices of the twin chains merge at certain parameter values. Figures 2(a) and (b) show, respectively, reconnecting period-two twin chains and reconnecting period-three twin chains. For the QNM, the merging of even-periodic twin chains is accompanied by a collision of periodic points as shown in Fig. 2(a), while odd-periodic twin chains merge without a collision of periodic points as shown in Fig. 2(b).

The QNM has already been studied to some extent. For instance, Howard and Hohs studied reconnection phenomena for the QNM, and pointed out the close relationship between the merging of the separatrices and the onset of global

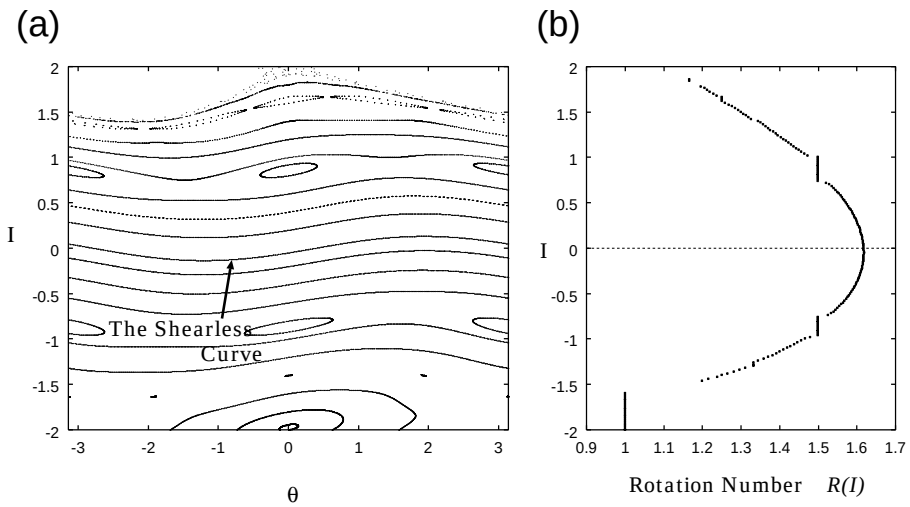

Fig. 1. (a) The phase space portrait of the QNM and (b) the rotation number profile along the I-axis, at $\mu = 1.62$, $K = 0.25$.

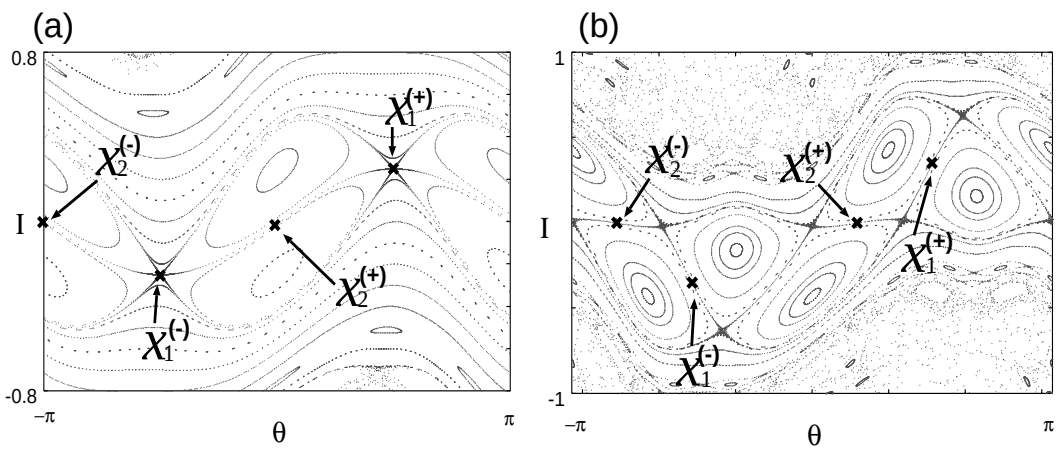

Fig. 2. (a) Reconnecting period-two twin chains at $\mu = -0.4900528$, $K = 0.5$. (b) Reconnecting period-three twin chains at $\mu = -0.3124513$, $K = 0.7$.

chaos.[3] On the other hand, using Greene's residue method, del-Castillo-Negrete et al. determined the critical parameter values for the breakup of the shearless KAM curve which has the rotation number given by the inverse golden mean, $1/\gamma\,(\gamma = (\sqrt{5}-1)/2)$.[7] The persistence of the shearless KAM curve with a Diophantine rotation number has been theoretically studied by Delshams and de la Llave.[12] Moreover, in our previous papers, we defined the indicator points for the QNM, and succeeded in systematically studying reconnection phenomena and obtaining the diagram for the onset of global chaos.[8),9)]

§3. The indicator points for the quadratic nontwist map

The mapping T can be rewritten as a product of two involutions, that is, $T = M_2 M_1$, with $M_1^2 = M_2^2 = 1$, where M_1 and M_2 are defined by

$$M_1 : \begin{cases} I' = I - K\sin(\theta) \\ \theta' = -\theta, \end{cases} \tag{6}$$

$$M_2 : \begin{cases} I' = I \\ \theta' = -\theta + 2\pi\mu - I^2. \end{cases} \tag{7}$$

Further, the mapping T commutes with the mapping S defined by

$$S : \begin{cases} I' = -I \\ \theta' = \theta + \pi. \end{cases} \tag{8}$$

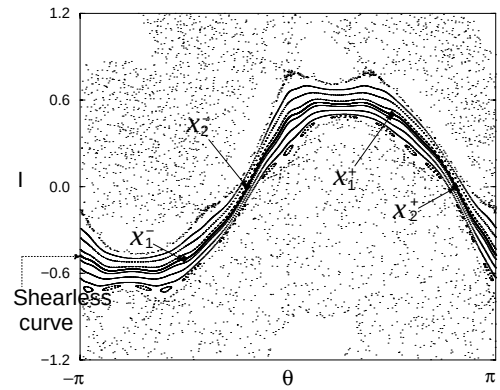

Fig. 3. The phase space portrait at $\mu = 0.304348$, K=1.0. The shearless KAM curve goes through the four indicator points.

Previously, we showed that if there exists a shearless KAM curve, then it is an invariant set of both the mapping T and the mapping S, and that the invariant set contains the solutions of the following equations:[8),9)]

$$M_1 \boldsymbol{x} = S\boldsymbol{x}, \tag{9}$$

$$M_2 \boldsymbol{x} = S\boldsymbol{x}. \tag{10}$$

The solutions of Eqs. (9) and (10) are given, respectively, by

$$\boldsymbol{x}_1^{(\pm)} = \left(\theta_1^{(\pm)},\, I_1^{(\pm)}\right) = \left(\pm\frac{\pi}{2},\, \pm\frac{K}{2}\right), \tag{11}$$

and

$$\boldsymbol{x}_2^{(\pm)} = \left(\theta_2^{(\pm)},\, I_2^{(\pm)}\right) = \left(\pi\left(\mu \pm \frac{1}{2}\right),\, 0\right). \tag{12}$$

Note that the relations $\boldsymbol{x}_j^{(\pm)} = S\boldsymbol{x}_j^{(\mp)}$ $(j = 1, 2)$ hold. We call these four points, $\boldsymbol{x}_1^{(+)}$, $\boldsymbol{x}_1^{(-)}$, $\boldsymbol{x}_2^{(+)}$, $\boldsymbol{x}_2^{(-)}$, the "indicator points" for the QNM, since we can derive useful information from the behavior of their trajectories. The properties of the indicator points are summarized as follows:

(i) when there exists a shearless KAM curve, it goes through the four indicator points as shown in Fig. 3;

(ii) when the separatrices of even-periodic twin chains merge, two of the four indicator points are periodic and the remaining indicator points are located on the separatrix of the twin chains as shown in Fig. 2(a);

(iii) when the separatrices of odd-periodic twin chains merge, all of the four indicator points are located on the separatrix of the twin chains as shown in Fig. 2(b).

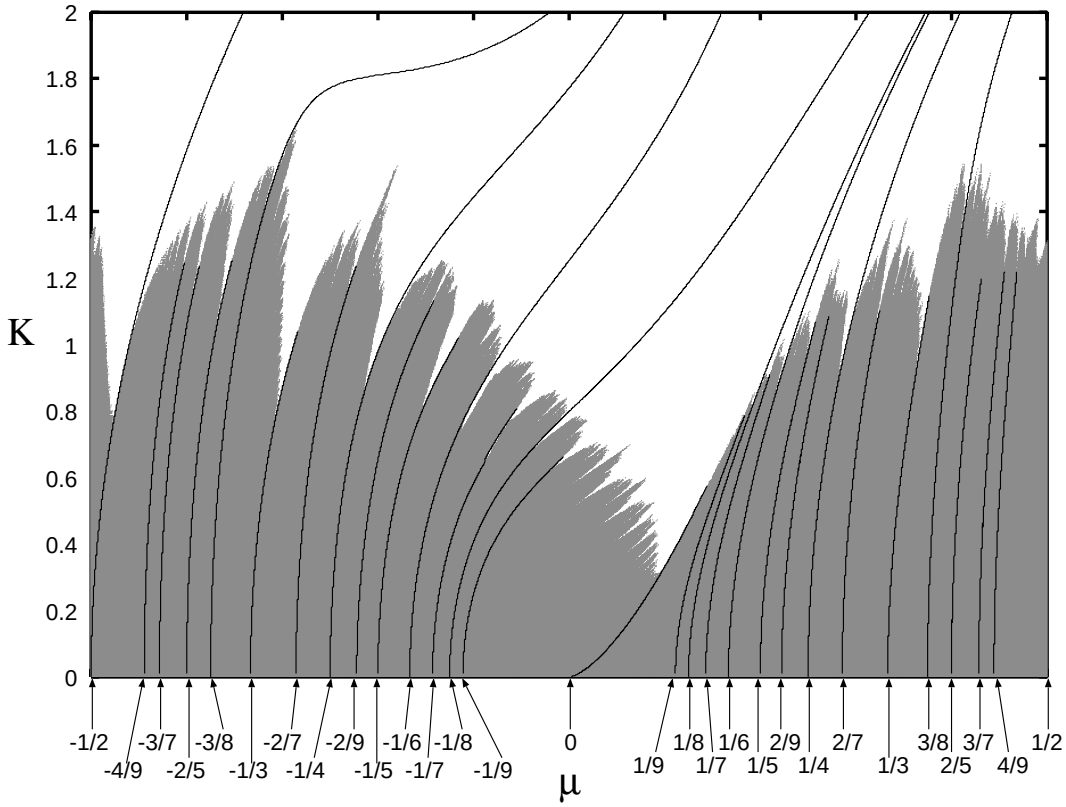

Fig. 4. The diagram for the onset of global chaos and the reconnection threshold curves for twin chains with various rotation numbers. The fractions below the μ-axis represent the rotation numbers of twin chains.

§4. The critical boundary and the reconnection thresholds

Using the indicator points, one can determine the critical boundary for the entire parameter plane, i.e. the μ-K plane. The critical boundary is a set of parameter values at which the last KAM curve breaks up. Here we review how the critical boundary can be obtained. As shown in Fig. 3, the KAM curves around the indicator points are typically robust. Thus, when the trajectories of the indicator points remain bounded, the following two cases are possible: (a) The shearless KAM curve exists, and the trajectories are confined on it (see Fig. 3), or (b) the shearless KAM curve does not exist, but the trajectories are confined in a narrow region bounded by KAM curves (see Fig. 2(b)). In either case, there exists at least one KAM curve in the phase space. That is, the bounded trajectories guarantee the existence of a KAM curve, whereas the unbounded trajectories obviously guarantee the nonexistence of a KAM curve. Therefore, one can assume that there exists at least one KAM curve if and only if the trajectories of the indicator points remain bounded.

For each set of μ and K, we numerically iterated the indicator points 10^5 times, and determined whether the trajectories remained bounded or not.[8] The result is

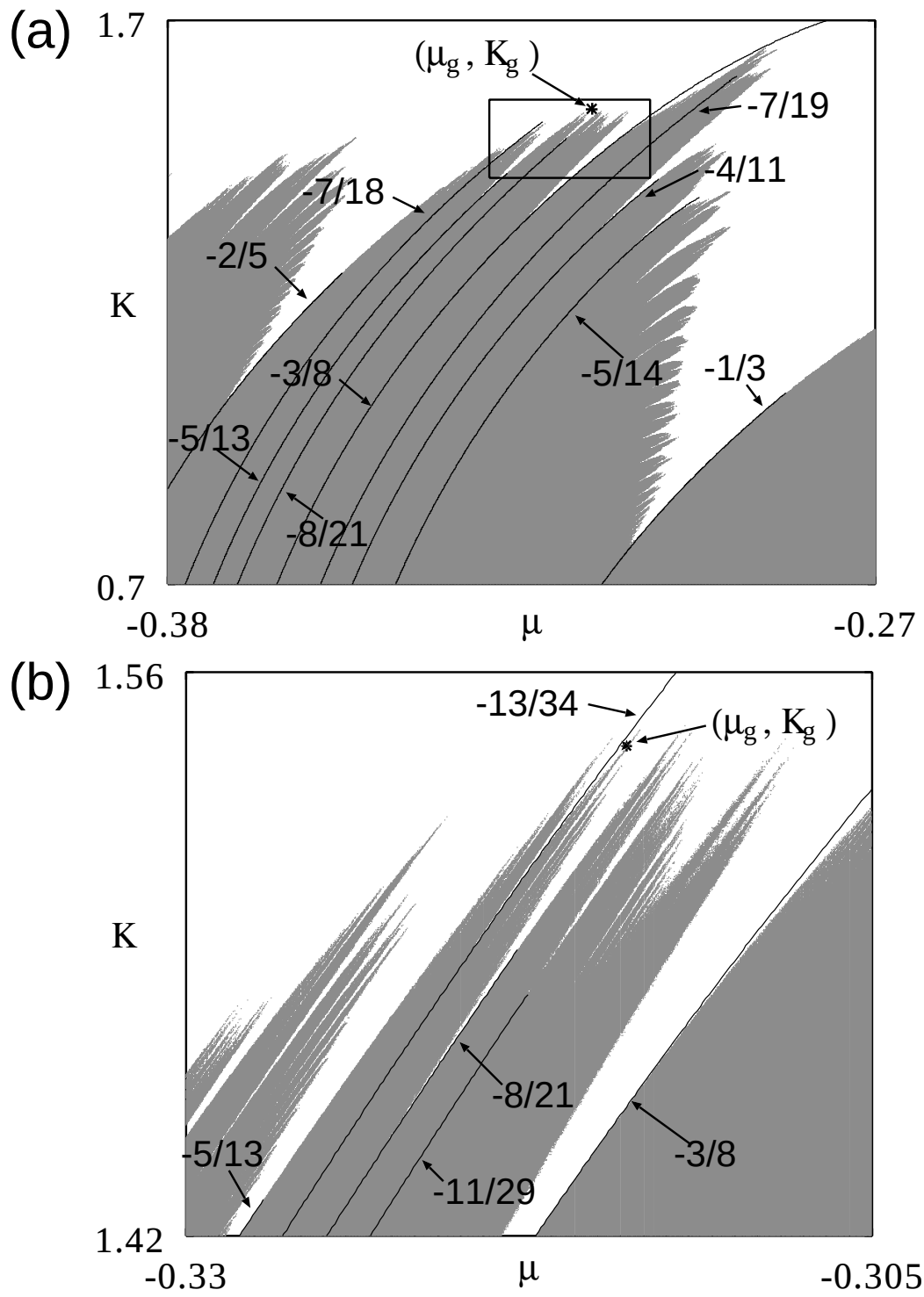

Fig. 5. (a) Magnification of the diagram around the critical point (μ_g, K_g). (b) Magnification of the box in (a) The reconnection threshold curves are also displayed. The fractions represent the rotation numbers of twin chains.

shown in Fig. 4, where the trajectories are bounded in the gray region, but are unbounded in the white region. Thus, the boundary between the gray and the white region in Fig. 4 corresponds to the critical boundary.

Further, the indicator points can be used to accurately determine the reconnection thresholds, i.e., the parameter values at which the separatrices of twin chains merge. For the determination of the reconnection thresholds for even-periodic twin chains, we use the periodic property of the indicator points, i.e. property *(ii)* mentioned above. On the other hand, in the cases of odd-periodic twin chains, we use the convergent property of the indicator points, i.e. property *(iii)* mentioned above. Employing the indicator points, we computed the reconnection thresholds for twin chains with periods less than or equal to 9.[8] These reconnection thresholds are superimposed onto the critical boundary as shown in Fig. 4. Because of numerical limitations, the reconnection thresholds for odd-periodic twin chains could not be computed in the globally chaotic regime.

The superposition of the critical boundary and the reconnection threshold curves reveals that the reconnection threshold curves determine the structure of the critical boundary. More precisely, the singularities of the critical boundary have a one-to-one correspondence with the reconnection threshold curves, and, for each singularity, a segment of the reconnection threshold curve agrees well with that of the critical boundary. These features can be more clearly confirmed for the magnification of small regions of the diagram, which will be presented below.

Using Greene's residue method, del-Castillo-Negrete et al. accurately determined the critical parameter values for the breakup of the shearless KAM curve with the inverse golden mean rotation number as $(\mu_g, K_g) \simeq (-0.313951, 1.54156)$.[7] Magnification of the critical boundary around this critical point is shown in Figs. 5(a) and (b), where the reconnection threshold curves for some twin chains with large periods are also displayed. Figures 5(a) and (b) suggest that the critical boundary reveals ever finer structure under magnification, that is, the critical boundary is a fractal.

§5. The last KAM curve for the QNM

It is of interest to ask what the rotation number of the last KAM curve is at each point of the critical boundary, and whether the shearless KAM curve is the last one to breakup or not. Only for the critical point (μ_g, K_g), a definitive answer has been given. Namely, it is numerically confirmed that when one increases the parameter values keeping the rotation number of the shearless KAM curve fixed at $1/\gamma$, the shearless KAM curve breaks up last at $\mu = \mu_g$, $K = K_g$.[7] In fact, the critical boundary displayed in Fig. 5(b) appears to contain the point (μ_g, K_g). Since the fine structure around the critical point (μ_g, K_g) displayed in Figs. 5(a) and (b) is a typical one for the critical boundary, we expect that the shearless KAM curve with an irrational rotation number other than $1/\gamma$ might also be the last KAM curve for an appropriate increase of the parameter values.

In order to verify the above conjecture, we numerically computed the rotation number ν of the indicator points for each point $(\tilde{\mu}, \tilde{K})$ of the critical boundary, where

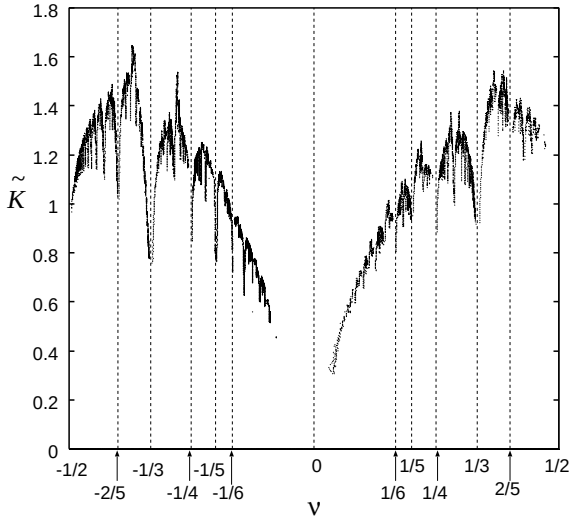

Fig. 6. The relation between the rotation number ν of the indicator points and the parameter $\tilde{K}$.

ν is defined by

$$\nu = \lim_{N\to\infty} \nu_N, \quad \nu_N = \frac{1}{2\pi N}\sum_{n=1}^{N}(\theta_n - \theta_{n-1}) \tag{13}$$

with the initial point, (θ_0, I_0), being one of the four indicator points defined by Eqs. (11) and (12). Note that the convergence of ν_N to a certain irrational value ensures the existence of the shearless KAM curve at the onset of global chaos. We numerically confirmed the convergence of ν_N for many points of the critical boundary, and obtained the relation between ν and $\tilde{K}$ as shown in Fig. 6. The function $\tilde{K}(\nu)$ suggests that there exist lots of irrational rotation numbers with which the shearless KAM curve breaks up last. It will be interesting to examine for what class of irrational rotation numbers the shearless KAM curve breaks up last. The detailed study on this problem will be reported elsewhere.

References

1) J. Moser, Nachr. Akad. Wiss. Göttingen, Math. -phys. **K1**, 11a (1962), 1.
2) J. N. Mather, Topology **21** (1982), 457.
S. Aubry and P. Y. LeDaeron, Physica **D8** (1983), 381.
3) J. E. Howard and S. M. Hohs, Phys. Rev. **A29** (1984), 418.
4) J. E. Howard and J. Humpherys, Physica **D80** (1995), 256.
5) J. P. Van der Weele, T. P. Valkering, H. W. Capel and T. Post, Physica **A153** (1988), 283.
6) J. P. Van der Weele and T. P. Valkering, Physica **D169** (1990), 42.
7) D. del-Castillo-Negrete, J. M. Greene and P. J. Morrison, Physica **D91** (1996), 1.
D. del-Castillo-Negrete, J. M. Greene and P. J. Morrison, Physica **D100** (1997), 311.
8) S. Shinohara and Y. Aizawa, Prog. Theor. Phys. **97** (1997), 379.
9) S. Shinohara and Y. Aizawa, Prog. Theor. Phys. **100** (1998), 219.
10) C. Simó, Regular and Chaotic Dynamics **3** (1998), 180.
11) H. R. Dullin, J. D. Meiss and D. Sterling, preprint (1999).
12) A. Delshams and R. de la Llave, preprint (1998).